c-Jun N-terminal kinase (JNK)-mediated modulation of brain mitochondria function: new target proteins for JNK signalling in mitochondrion-dependent apoptosis

Hagen SCHROETER*, Clinton S. BOYD*, Ruhi AHMED*, Jeremy P. E. SPENCER†, Roger F. DUNCAN*, Catherine RICE-EVANS† and Enrique CADENAS*[1]

*Department of Molecular Pharmacology and Toxicology, School of Pharmacy, University of Southern California, 1985 Zonal Avenue, Los Angeles, CA 90089-9121, U.S.A., and †Wolfson Centre for Age-Related Diseases, School of Biomedical Sciences, King's College, London SE1 9RT, U.K.

The molecular mechanisms underlying the initiation and control of the release of cytochrome c during mitochondrion-dependent apoptosis are thought to involve the phosphorylation of mitochondrial Bcl-2 and Bcl-x_L. Although the c-Jun N-terminal kinase (JNK) has been proposed to mediate the phosphorylation of Bcl-2/Bcl-x_L the mechanisms linking the modification of these proteins and the release of cytochrome c remain to be elucidated. This study was aimed at establishing interdependency between JNK signalling and mitochondrial apoptosis. Using an experimental model consisting of isolated, bioenergetically competent rat brain mitochondria, these studies show that (i) JNK catalysed the phosphorylation of Bcl-2 and Bcl-x_L as well as other mitochondrial proteins, as shown by two-dimensional isoelectric focusing/SDS/PAGE; (ii) JNK-induced cytochrome c release, in a process independent of the permeability transition of the inner mitochondrial membrane (imPT) and insensitive to cyclosporin A; (iii) JNK mediated a partial collapse of the mitochondrial inner-membrane potential ($\Delta\psi$m) in an imPT- and cyclosporin A-independent manner; and (iv) JNK was unable to induce imPT/swelling and did not act as a co-inducer, but as an inhibitor of Ca-induced imPT. The results are discussed with regard to the functional link between the $\Delta\psi$m and factors influencing the permeability transition of the inner and outer mitochondrial membranes. Taken together, JNK-dependent phosphorylation of mitochondrial proteins including, but not limited to, Bcl-2/Bcl-x_L may represent a potential of the modulation of mitochondrial function during apoptosis.

Key words: Bax, Bcl-2, cytochrome c, membrane potential, phosphorylation, proteome.

INTRODUCTION

The ability to execute apoptosis is an evolutionarily conserved physiological process responsible for the elimination of redundant or injured cells in multicellular organisms [1]. However, the anomalous regulation of apoptosis has been recognized as a pathological process that occurs in a variety of conditions comprising neurodegenerative diseases, autoimmune disorders and various cancers [1–3]. Consequently, the understanding of regulation and execution of apoptosis may deliver tools for the prevention or therapy of several diseases.

Apoptosis may be executed via two predominant effector pathways, which eventually converge at the level of caspase-3 activation [1]. First, the death-receptor pathway, which is initiated by members of the death-receptor superfamily and leads to the recruitment and subsequent activation of pro-caspase-8 through the formation of active adaptor molecules, such as Fas-associated death-domain protein ('FADD') [1]. Secondly, the mitochondrial pathway, characterized by the release of pro-apoptotic proteins, such as cytochrome c, the formation of the apoptosome [a complex consisting of pro-caspase-9, apoptosis protease-activating factor-1 (Apaf-1), cytochrome c and ATP/deoxyATP] and the succeeding activation of pro-caspase-9. Both pathways finally lead to the activation of caspase-3 and the subsequent proteolytic cleavage of apoptotic substrates [1].

In this scheme of events, the Bcl-2 family of proteins is integral at a crucial point upstream of irrevocable cellular damage. In general, the Bcl-2 family consists of inhibitors (most commonly Bcl-2 and Bcl-x_L) and promoters (Bax, Bad, Bid and others) of apoptosis, equally competent in modulating both effector pathways [1,3–5]. In addition, Bcl-2 proteins may facilitate crosstalk between the death receptor and mitochondrial pathways via the pro-apoptotic protein Bid [1,4,5].

Unlike Bcl-2 and Bcl-x_L, which exist typically attached to intracellular membranes, other Bcl-2 family members, including Bax, Bad and Bid, form cytosolic pools of inactive proteins [1,4,5]. Following an apoptotic stimulus, these proteins are transformed into their active conformation and translocate to membranes of target organelles, such as the mitochondria, where they are thought to facilitate apoptosis by mediating the release of apoptotic proteins [6]. The activity or function of all known Bcl-2 family proteins is regulated by means of protein dimerization, proteolytic cleavage or post-translational modification, especially phosphorylation [1,4–6].

Although the anti-apoptotic properties of Bcl-2 and Bcl-x_L have been characterized in various cell-culture systems [4] and *in vivo* [7], the molecular mechanisms underlying these effects are diverse and often unclear. One potential explanation favours the notion that Bcl-2 and Bcl-x_L directly heterodimerize with pro-apoptotic members of the Bcl-2 family and thus neutralize detrimental effects [4,8]. Other suggestions argue that Bcl-2 and Bcl-x_L indirectly modulate the activities of pro-apoptotic Bcl-2 members by interfering with essential organelle targeting or membrane-integration processes [1,4]. Furthermore, the binding of Bcl-2 and Bcl-x_L to proteins involved in the regulation of mitochondrial function, such as the voltage-dependent anion channel (VDAC) [9] or the adenine nucleotide translocase (ANT) [10], has been suggested and may provide an alternative explanation. The emerging picture strengthens the concept that the participation of Bcl-2 and Bcl-x_L in protein–protein interactions with either other Bcl-2 family members or different target proteins provides the basis for their anti-apoptotic properties.

It may be hypothesized that post-translational modifications, such as phosphorylation, are likely to attenuate or intensify the anti-apoptotic properties of Bcl-2/Bcl-x_L [11–14]. In this respect, the majority of published observations seem to favour the hypothesis that phosphorylation of Bcl-2 parallels inactivation [11,13,14], thus promoting apoptosis. Conversely, separate lines of evidence indicate that the phosphorylation of Bcl-2 is required for the full anti-apoptotic function of Bcl-2 [12]. Other authors describe the phosphorylation of Bcl-2 as a physiological response to mitotic progression [15] or fail to correlate Bcl-2 phosphorylation with other functional consequences [4,5].

Due to the fact that a variety of different stimuli have mediated apoptosis coinciding with Bcl-2 phorphorylation, various kinases including Raf-1 [16], CDC2/cyclin B1 [17], cAMP-dependent protein kinase [18] and extracellular signal-regulated kinase (ERK) [19] have been investigated. The results of these studies seemingly exclude these proteins as Bcl-2 kinases. Nevertheless, it has been established that the c-Jun N-terminal kinase (JNK), an important mediator of apoptotic responses [20], facilitates the phosphorylation of Bcl-2 and Bcl-x_L in different cell-culture systems and in response to a variety of stimuli [14,19,22,23]. However, the conclusion that JNK-mediated phosphorylation inhibits the pro-survival effects of Bcl-2 remains controversial. Some reports indicate that phosphorylation of Bcl-2 enhances anti-apoptotic properties [12] and possibly modulates ubiquitin-mediated degradation of Bcl-2 [24], consequently altering its biological half-life, thus producing anti-apoptotic effects. Experiments in cell-culture systems, however, may be unsuitable to elucidate whether JNK either directly catalyses Bcl-2/Bcl-x_L phosphorylation or facilitates this response through the activation of other, as yet unknown, mediator kinases. It may be surmised that the mechanism and function of Bcl-2 phosphorylation remains controversial and that the particular processes involved in JNK-mediated pro-apoptotic responses directed towards the mitochondria are just beginning to emerge.

The purpose of this study was to clarify the potential biological role of mitochondria as an important cellular target of pro-apoptotic JNK signalling. To address this problem, we studied the effect of active dual-phosphorylated recombinant JNK1 as well as active immunoprecipitated JNK on isolated coupled and bioenergetically competent brain mitochondria and posed the following questions. (i) Does JNK catalyse Bcl-2/Bcl-x_L phosphorylation directly? (ii) Do other target proteins for JNK exist within mitochondria? (iii) Does JNK mediate the release of pro-apoptotic factors and does this involve mitochondrial inner-membrane permeability transition (imPT) and/or mitochondrial

outer-membrane permeability transition (omPT)? (d) Does JNK facilitate changes in the bioenergetic parameters of mitochondria?

The results of this study support the notion that mitochondrially directed JNK signalling might be essential for the execution of apoptotic processes by mechanisms involving the phosphorylation of Bcl-2/Bcl-x_L as well as other mitochondrial proteins.

EXPERIMENTAL

Materials

Recombinant active and inactive JNK1 and ERK1/2, glutathione S-transferase (GST)–activating transcription factor 2 (ATF-2), GST–c-Jun and P81 paper were purchased from Upstate Biotechnology (Waltham, MA, U.S.A.). [γ-^{32}P]ATP, the ECL-Plus-detection system, Hybond blotting paper and nitrocellulose/PVDF membranes were obtained from Amersham Biosciences (Piscataway, NJ, U.S.A.). Nonidet P-40 and CHAPS were bought from Pierce (Rockford, IL, U.S.A.). Ampholines and SYPRO™ Ruby protein gel stain were purchased from Bio-Rad (Hercules, CA, U.S.A.) and Molecular Probes (Eugene, OR, U.S.A.), respectively. All other chemicals or reagents were obtained from Sigma-Aldrich (St Louis, MO, U.S.A.) or Calbiochem (La Jolla, CA, U.S.A.).

Isolation of rat brain mitochondria

Adult male Wistar rats (6 months old), housed under an automated light/dark (12 h:12 h) cycle with food and water available *ad libitum*, were fasted overnight and killed by cervical dislocation. All experimental procedures were subject to the approval of the Institutional Animal Care and Use Committee (IACUC) of the University of Southern California, Los Angeles, CA, U.S.A. The brains were excised, rinsed in ice-cold saline, and cerebellum, brainstem and pineal gland were removed. The remaining tissue was pooled and homogenized in ice-cold buffer, pH 7.4, containing sucrose (250 mM), Hepes (20 mM), EDTA (1 mM), EGTA (1 mM), dithiothreitol (DTT; 1 mM), PMSF (1 mM), leupeptin (5 μg/m) and aprotinin (25 μg/ml) using a Dounce homogenizer to give a 5 % (w/v) homogenate. Non-synaptosomal mitochondria were isolated by differential centrifugation followed by discontinuous Percoll density-gradient centrifugation, according to procedures described previously [25] with modifications. All procedures were performed at 4 °C. Briefly, the homogenate was centrifuged at 1400 *g* for 3 min (Eppendorf 5810R centrifuge) to remove nuclei and cell debris. The supernatant was centrifuged at 21000 *g* for 10 min (Eppendorf 5810R centrifuge), and the resultant pellet was resuspended in 15 % Percoll and layered on to a pre-formed discontinuous gradient of 23 %/40 % Percoll. The gradient was centrifuged at 31000 *g* for 10 min (Beckman Coulter Optima XL-80K Ultracentrifuge). Mitochondrial fractions were collected, subsequently diluted 1:4 in mitochondrial isolation buffer (MIB), pH 7.4, containing sucrose (250 mM), Hepes (20 mM), EDTA (1 mM), EGTA (1 mM), DTT (1 mM), PMSF (1 mM), leupeptin (2 μg/ml) and aprotinin (10 μg/ml), and centrifuged at 17000 *g* for 10 min (Eppendorf 5810R centrifuge). The resulting pellet was treated in MIB supplemented with 0.5 mg of BSA/ml and then washed twice in BSA-free MIB using centrifugation at 11000 *g* for 10 min (Eppendorf 5810R centrifuge). The final mitochondrial pellet was resuspended in MIB to obtain a protein concentration of 1 mg/ml. Mitochondrial integrity was determined by measuring oxygen uptake with a Clark-type electrode (Oxygraph 32; Hansatech Instruments, King's Lynn, Norfolk, U.K.). The ratio of

ADP-stimulated (state 3) respiration to resting (state 4) respiration, known as the respiratory control ratio (RCR), was measured using succinate (a complex II respiratory substrate) and rotenone (a complex I inhibitor) to assess the structural and bioenergetical integrity of isolated mitochondria.

The purity of the mitochondrial fraction was assessed as follows. First, the activities of glucose-6-phosphatase and NADPH-cytochrome c reductase as markers for microsomal contamination were measured using the methods of Swanson [26] and Sottocasa et al. [27], respectively. Secondly, the presence of synaptosomal, i.e. cytosolic, contaminations was assessed by measuring the lactate dehydrogenase activity as described previously [28]. Thirdly, nuclear and cytosolic contaminations were evaluated by the absence of the proliferating cell nuclear antigen (PCNA) and β-actin as determined by immunoblot analysis (described below), respectively.

The effect of active JNK on functional parameters of isolated brain mitochondria

Functional proteomics

Mitochondria (100 μg) were apportioned in mitochondria kinase buffer (MKB), containing MIB supplemented with ATP (0.6 mM) or [γ-^{32}P]ATP (10 μCi/vial; 6000 Ci/mmol), β-glycerophosphate (25 mM) and MgCl (10 mM), and energized with succinate (5 mM). Mitochondria were treated with 0.3 μg of active dual-phosphorylated recombinant JNK1 (arJNK1), 0.3 μg of inactive non-phosphorylated recombinant JNK1 (rJNK1) or 0.7 μg of active immunoprecipated JNK (aipJNK) and incubated for 30 min at 37 °C under gentle agitation. Following this incubation and three washing steps, mitochondria and supernatant were separated by centrifugation (4000 g, 5 min), collected and prepared for immunoprecipitation of Bcl-2/Bcl-x$_L$, two-dimensional isoelectric focusing (2D IEF)/SDS/PAGE or SDS/PAGE and immunoblotting as described below.

Membrane potential

The effect of JNK on the mitochondrial inner-membrane potential ($\Delta\psi$m) was assessed as described previously [29] by measuring the $\Delta\psi$m-dependent distribution of the fluorescent probe tetramethylrhodamine methyl ester (TMRM) using a Perkin-Elmer LS 55 luminescence spectrometer. Mitochondria were suspended in MKB containing TMRM (0.5 μM), rotenone (5 μM) and oligomycin (5 μM), energized with succinate (5 mM), and incubated with 0.3 μg of arJNK1/rJNK1 or 0.7 μg of aipJNK in the presence or absence of cyclosporin A (CsA; 5 μM) for 30 min at 37 °C. The protonophore carbonyl cyanide p-trifluoromethoxyphenylhydrazone (FCCP; 0.5 μM) was added at the end of each experiment to collapse $\Delta\psi$m to serve as an internal control.

Permeability transition

The effect of JNK on calcium-induced mitochondrial permeability transition was assessed by monitoring the decrease in absorption at 540 nm. Mitochondria were suspended in buffer, pH 7.4, containing mannitol (220 mM), sucrose (68 mM), Hepes (10 mM), KH$_2$PO$_4$ (5 mM), NaCl (2 mM), succinate (5 mM), ATP (2 mM), MgCl (2 mM), creatine kinase (75 μg/ml), phosphocreatine (10 mM) and rotenone (5 μM). This buffer is designed to mimic biologically relevant ATP concentrations outside of mitochondria (i.e. on the cytosolic side). Compared with other buffer systems used to assess mitochondrial swelling, this approach takes into account that ATP may play an important role during permeability transition, due to its influence on the conformation of the ANT. As a result, the Ca^{2+} concentration required for inducing permeability transition may be more closely related to biological systems [30] and may be higher compared with swelling buffers in which ATP is omitted. Mitochondria were treated with CaCl$_2$ (150 μM; positive control) or arJNK1/rJNK1/aipJNK in the presence or absence of CsA (5 μM) or FCCP (0.5 μM).

Immunoprecipitation

Primary cortical neurons were cultured as described previously [31]. Low-density lipoprotein was isolated in accordance with the approved procedures of the University of Southern California Institutional Review Board and oxidized as detailed in [32]. Lysates derived from cultured primary cortical neurons, treated with oxidized low-density lipoprotein as described in [32], were used to immunoprecipitate active JNK. In brief, cells were lysed in immunoprecipitation buffer, pH 7.5, containing Tris/HCl (20 mM), NaCl (150 mM), Nonidet P-40 (1 %), SDS (0.1 %), EDTA (2 mM), EGTA (2 mM), phosphatase inhibitors NaF (50 mM), sodium orthovandanate (1 mM) and sodium pyrophosphate (2 mM), and protease inhibitors PMSF (1 mM), antipain (20 μg/ml), leupeptin (10 μg/ml), pepstatin (5 μM), chymostatin (10 μM) and aprotinin (5 μg/ml). The soluble protein fraction was incubated with anti-JNK1 polyclonal antibody (pAb; Santa Cruz Biotechnology) overnight at 4 °C and precipitated with Protein G-Plus-Agarose (Santa Cruz Biotechnology) for 60 min. The resulting immunocomplex was analysed by immunoblotting using anti-(ACTIVE JNK) pAb (Promega) and the JNK activity was measured as described below.

Bcl-2 and Bcl-x$_L$ were immunoprecipitated from the mitochondria treated with arJNK1/rJNK1/aipJNK in [γ-^{32}P]ATP containing MKB as described above. Mitochondria were lysed in immunoprecipitation buffer by sonication (5 × 10 s; Branson Sonifier 250) and vortex mixing (3 × 10 s) on ice. The lysates were centrifuged for 15 min at 14000 g at 4 °C, the supernatant was collected and cleared with Protein A–agarose [Santa Cruz Biotechnology; 25 μl of 25 % (v/v) suspension/ml] for 30 min at 4 °C. Thereafter, the supernatants were incubated with either anti-(Bcl-2-AC) antibody or anti-Bcl-x$_L$ antibody (both from Santa Cruz Biotechnology) overnight at 4 °C under gentle agitation. Bcl-x$_L$ immunocomplexes were captured with Protein G-Plus-Agarose for 2 h at 4 °C and subsequent centrifugation (1500 g, 60 s, 4 °C). Bcl-2 immunocomplexes were obtained by centrifugation (1500 g, 60 s, 4 °C). Immunocomplexes were solubilized in SDS sample buffer, separated using Laemmli SDS/PAGE (12 % gel) and analysed by autoradiography.

Western immunoblotting and 2D IEF/SDS/PAGE

Mitochondrial and supernatant fractions obtained following treatment with arJNK1/rJNK1/aipJNK as described above were solubilized in SDS sample buffer, separated by Laemmli SDS/PAGE (10, 12 or 15 % gels) and immunoblotted with anti-β-actin antibody, anti-(heat-shock protein 70) (Hsp70) pAb, anti-Hsp60 pAb, anti-Bcl-2 pAb, anti-Bcl-x$_L$ pAb, anti-Bax pAb, anti-(cytochrome c) pAb, anti-(apoptosis-inducing factor) pAb, anti-Smac (second mitochondria-derived activator of caspases; also known as DIABLO) pAb and anti-(phospho-Tyr) antibody (all from Santa Cruz Biotechnology).

For 2D IEF/SDS/PAGE, mitochondrial pellets obtained following treatment with arJNK1/rJNK1/aipJNK, as described above, were solubilized in a two-step procedure to ensure the efficient breakdown of mitochondrial membranes, complete reduction of disulphide bonds and effective dissociation of protein–lipid interactions. First, the mitochondrial pellet was solubilized by heating the sample in buffer, pH 10, containing SDS (1 % w/v), DTT (100 mM), sodium orthovandanate (1 mM) and CHAPS (60 mM) at 95 °C for 5 min. Following this step, the solution was vortex mixed, cooled rapidly to room temperature and urea and thiourea were added to final concentrations of 7 and 2 M respectively. Thereafter, an equal volume of two-dimensional gel sample buffer, containing urea (7 M), thiourea (2 M), Triton X-100 (10 %), Nonidet P-40 (2 %), CHAPS (60 mM), DTT (70 mM) and ampholines pH range 3.5–10 (200 μl/ml; Bio-Rad), was added. The mixture was centrifuged at 10000 **g** for 5 min at room temperature and the supernatant was collected. The 2D IEF/SDS/PAGE of these supernatants was performed as described previously [33]. In the first dimension, 70 % pH 5–7/30 % pH 3.5–10 ampholines (Bio-Rad) were used and the second dimension was carried out using a 10.5 % acrylamide gel. Following 2D IEF/SDS/PAGE, the gels were analysed in two ways. Gels were stained with SYPRO™ Ruby protein gel stain in accordance with the protocol of the manufacturer (Molecular Probes) and images were acquired using a VersaDoc1000 imaging system (Bio-Rad). Thereafter, the gels were dried and an autoradiography was performed. Other gels were immunoblotted on to a PVDF membrane, probed with anti-Bcl-2 and anti-Bcl-x$_L$ pAbs and detected with horseradish peroxidase-conjugated secondary antibodies (Santa Cruz Biotechnology) and the ECL-Plus-detection system. In addition, Edman degradation was performed by the Microchemical Core Facility, Keck School of Medicine, University of Southern California, to identify certain peptides separated by 2D IEF/SDS/PAGE.

Assay for kinase activity and phosphorylation analysis

To assess the activity of the JNK used in these experiments, the phosphorylation of two major substrates, namely c-Jun and ATF-2, was investigated using [γ-^{32}P]ATP. In brief, GST–ATF-2 (5 μg/50 μl) or GST–c-Jun (5 μg/50 μl) were incubated in assay dilution buffer (Upstate Biotechnology) containing Mops (20 mM, pH 7.2), β-glycerophosphate (25 mM), EGTA (5 mM), MgCl (75 mM), sodium orthovandanate (1 mM) and DTT (1 mM) with ATP/[γ-^{32}P]ATP (0.5 mM; 50 μCi/vial) in the presence or absence of arJNK1/rJNK/aipJNK/inactive immunoprecipitated JNK (ipJNK) for 10 min at 30 °C under gentle agitation. Following incubation, 30 μl of each reaction mixture was applied on to the centre of a P81 paper square (2 cm^2), incubated for 60 s at room temperature and washed twice in 50 ml of phosphoric acid (0.75 %) for 5 min under agitation. Thereafter, each paper square was washed in 20 ml of acetone for 3 min, drained and counted by liquid scintillation spectroscopy (Beckman LS1801). The JNK activity was expressed as radioactivity in c.p.m., corrected for blanks and control values (substrates with ATP/[γ-^{32}P]ATP, but without JNK, and JNK with ATP/[γ-^{32}P]ATP, but without substrates).

To measure the ERK- or JNK-catalysed phosphorylation of mitochondrial proteins and recombinant His-tagged Bcl-2 (His-Bcl-2), 5 μg of His-Bcl-2 and 100 μg of isolated mitochondrial protein were incubated with arJNK1/rJNK1/aipJNK or recombinant active ERK1/recombinant active ERK2 and analysed as described above.

Table 1 Marker proteins and their activities in isolated rat brain mitochondria

Values represent means $\pm$ SD ($n = 3$). Assay conditions are described in the Experimental section.

Enzyme	Subcellular localization	Specific activity	
		Crude homogenate	Mitochondrial fraction
Lactate dehydrogenase*	Cytosolic/ synaptosomal	5.58 ± 0.27	0.12 ± 0.02
Glucose-6-phosphatase†	Microsomal	14.3 ± 1.1	0.01 ± 0.01
NADPH-cytochrome c reductase†	Microsomal	21.3 ± 1.2	0.04 ± 0.01

* Specific activity given as μmol/min per mg of protein.
† Specific activity given as nmol/min per mg of protein.

RESULTS

Isolation of rat brain mitochondria

Various kinases/phosphatases have been identified that catalyse the phosphorylation/dephosphorylation of a variety of mitochondrial proteins. Therefore, it ought to be considered that kinase/phosphatase activities functionally associated with cell membranes and cytoskeleton, cytosol, nuclear or microsomal cell fractions may influence the experimental outcome. The high purity of the rat brain mitochondria preparations used in these experiments was assessed by measuring the activities of the marker proteins lactate dehydrogenase (cytosolic, synaptosomal), glucose-6-phosphatase (microsomal) and NADPH-cytochrome c reductase (microsomal; Table 1). These activities were found to be close to the detection limit (Table 1). Western-blot analysis revealed that the mitochondrial fraction was devoid of immunodetectable β-actin (cytoskeletal marker) and the nuclear marker protein PCNA (results not shown). The ratio of ADP-stimulated (state 3) respiration to resting (state 4) respiration, known as the RCR, was measured using succinate (a complex II respiratory substrate) and rotenone (a complex I inhibitor). An RCR value of approx. 5 was obtained routinely.

JNK-mediated phosphorylation of mitochondrial proteins

As the known Bcl-2-phosphorylation sites conform to the established consensus motif for substrates of mitogen-activated protein kinases, including ERK and JNK, it was determined whether or not these kinases were capable of phosphorylating recombinant C-terminal His-tagged Bcl-2 or native Bcl-2 as contained within isolated rat brain mitochondria. The results obtained with recombinant active ERK1 and recombinant active ERK2 confirmed that ERK is not likely to play a role as a Bcl-2 kinase [14]. Due to the fact that a role for JNK as a Bcl-2-kinase was proposed earlier, experiments utilizing recombinant JNK as well as ipJNK were carried out. Active JNK from primary cortical neurons treated with oxidized low-density lipoprotein was obtained by immunoprecipitation (see the Experimental section). Analysis of the JNK immunocomplex by Western immunoblotting using anti-(ACTIVE JNK) pAb recognized two chromatographically distinct proteins exemplified by a major band at 46 kDa (probably p46^{JNK1}) and a less-intense band at 54 kDa (most likely p54^{JNK2}). No bands could by recognized in parallel experiments using immunocomplexes obtained from untreated control cultures. JNK immunoprecipitates from oxidized-low-density-lipoprotein-treated neurons, but not those
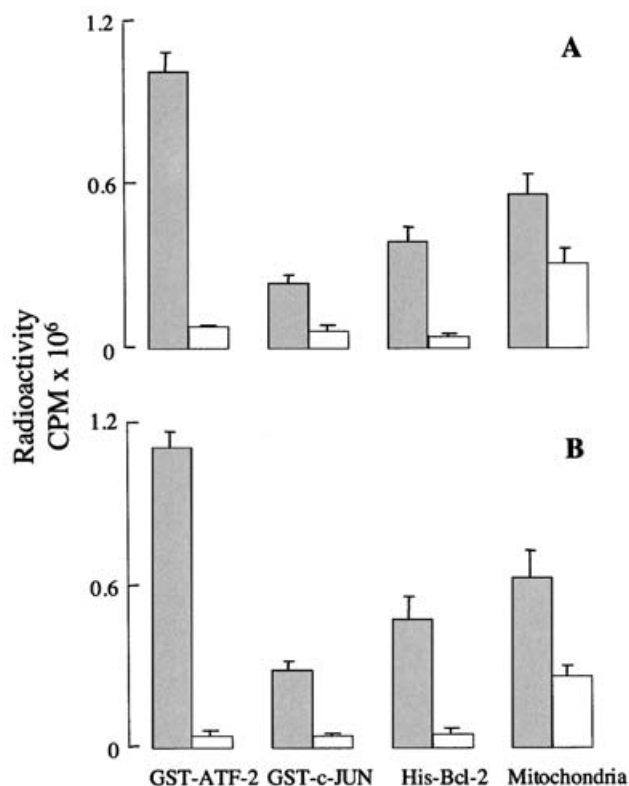
Figure 1   Activity of immunoprecipitated and recombinant JNK

Assay conditions as described in the Experimental section. (**A**) aipJNK (shaded bars) and (**B**) arJNK1 (shaded bars) were incubated with GST–ATF-2, GST–c-JUN (endogenous JNK substrate), recombinant C-terminal His-tagged Bcl-2 (His-Bcl-2) and isolated rat brain mitochondria in the presence of $[\gamma\text{-}^{32}P]$ATP. Control experiments using (**A**) ipJNK (white bars) and (**B**) rJNK1 (white bars) were carried out to account for non-specific binding. Data are representative of three independent experiments.

Figure 2   JNK-catalysed phosphorylation of mitochondrial Bcl-2 and Bcl-x$_L$

Assay conditions as described in the Experimental section. Rat brain mitochondria were incubated with arJNK1/rJNK1 and aipJNK in the presence of $\gamma\text{-}^{32}P$. Mitochondrial lysates were immunoblotted using anti-Bcl-2 (**A**) and anti-Bcl-x$_L$ (**B**) pAbs. In parallel experiments, Bcl-2 and Bcl-x$_L$ were immunoprecipitated from mitochondrial lysates and analysed by SDS/PAGE and autoradiography. Active JNK (arJNK1 and aipJNK), but not inactive JNK (rJNK1), is capable of phosphorylating mitochondrial Bcl-2 (**C**) and Bcl-x$_L$ (**D**).

from control cultures, catalysed the phosphorylation of the substrate proteins GST–ATF-2 and GST–c-Jun (Figure 1A).

For subsequent experiments, the specific activities of aipJNK and arJNK1 were standardized with regard to the integration of $[\gamma\text{-}^{32}P]$ATP in GST–ATF-2 to yield a radioactivity of approx. 10^6 c.p.m. following the standard kinase assay (see the Experimental section). Both aipJNK (Figure 1A) and arJNK1 (Figure 1B) were competent in catalysing the phosphorylation of Bcl-2 as well as mitochondrial proteins. It was established that isolated rat brain mitochondria contain Bcl-2 (Figure 2A) and Bcl-x$_L$ (Figure 2B) and, more importantly, that arJNK1 and aipJNK phosphorylate these proteins (Figures 2C and 2D).

Although the role of JNK with regard to the phosphorylation of mitochondrial proteins, especially Bcl-2 and Bcl-x$_L$, was investigated previously, little is known of other JNK targets within mitochondria. Therefore, 2D IEF/SDS/PAGE was used to examine the mitochondrial proteome for post-translational modifications caused by exposure of isolated mitochondria to active JNK (as detailed in the Experimental section, existing methods of sample preparation for 2D IEF were further developed into a two-step procedure to ensure the efficient breakdown of mitochondrial membranes, complete reduction of disulphide bonds and effective dissociation of protein–lipid interactions). Figure 3 shows a representative ($n=24$) digitalized image of a two-dimensional gel from rat brain mitochondrial proteins stained with SYPRO™ Ruby. On average, approx. 580 individual
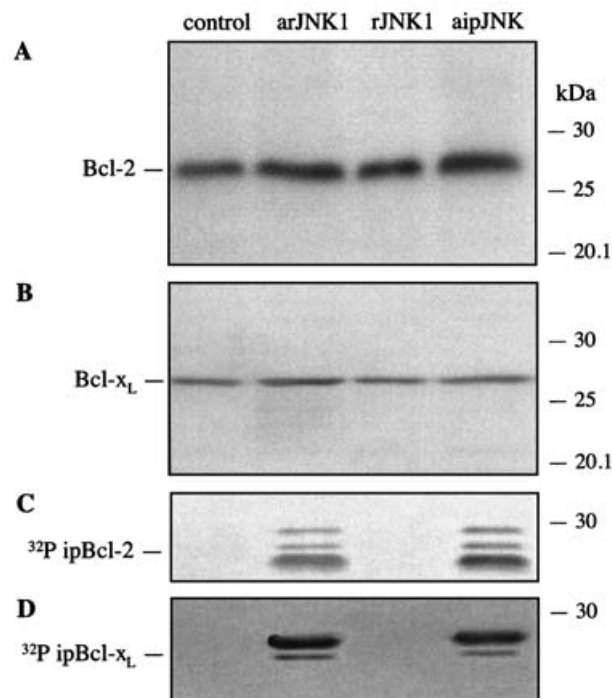
spots could be detected. In order to assign an approximate molecular mass and isoelectric point (pI) to individual protein spots, marker proteins with known mass and pI were used. In addition, to verify the data obtained from these marker proteins and to take into account local geometric distortion (often observed in two-dimensional gels), seven proteins were identified. The designations of these proteins as well as information with regard to localization within mitochondria are presented in Table 2. Figure 3 shows the resolution of mitochondrial proteins with regard to a defined molecular-mass separation ranging from 76 to 31 kDa and a defined pI separation in the pH range from 4.5 to 8.5. Collectively, this definition of the gel resolution allows a moderately accurate estimation of molecular mass and isolectric point for all present individual protein spots.

Analysis of the mitochondrial proteome by 2D IEF/SDS/PAGE following a 30 min incubation of isolated mitochondria in the presence of active JNK revealed no significant changes with regard to either the number or the densitometric characteristics of the spots detected when compared with controls. Thus $[\gamma\text{-}^{32}P]$ATP was utilized to radioactively label JNK substrate proteins present within mitochondria and 2D IEF/SDS/PAGE followed by autoradiography was used to investigate JNK-catalysed phosphorylation. Figure 4(A) shows a representative two-dimensional gel autoradiogram of control mitochondria ($n=6$) treated with inactive rJNK1. The results show several $\gamma\text{-}^{32}P$-labelled peptides of which the spots numbered 1, 2, 3 and 4 seem to be the predominant ones. The spots designated 1, 2 and 3 represent peptides with an approximate molecular mass of 55 kDa and are located in a pH range from 6.6 to
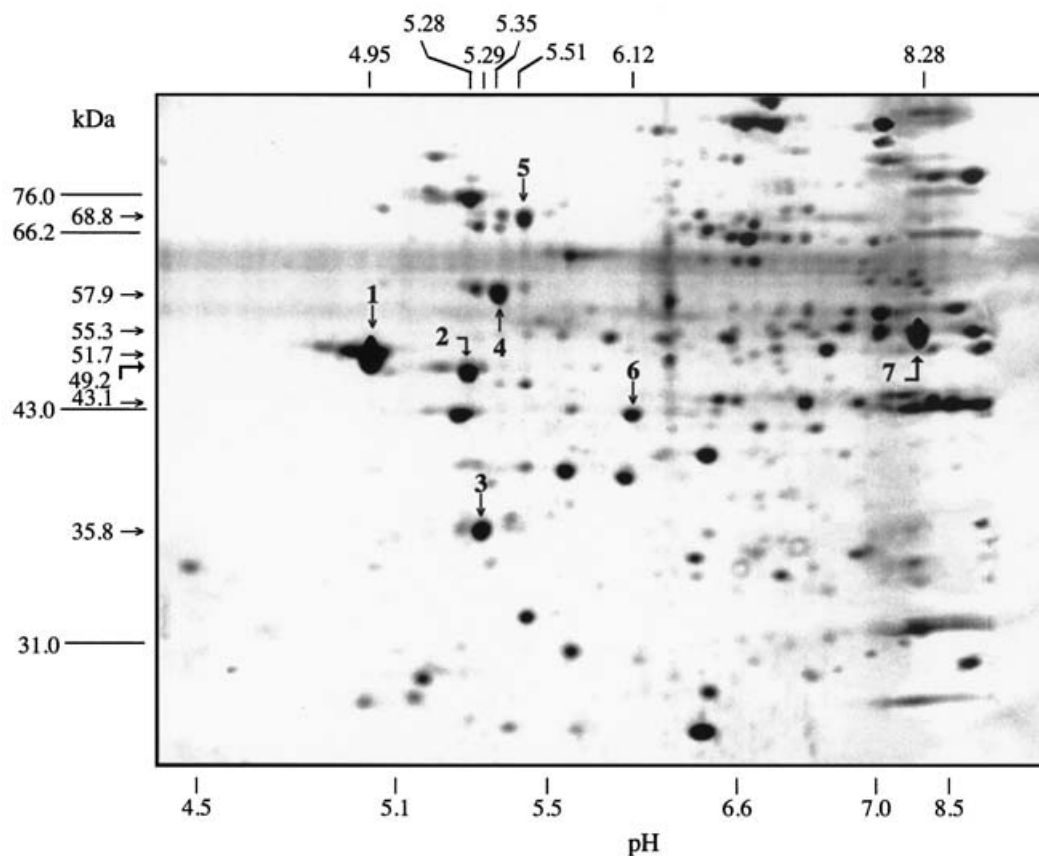
Figure 3   2D IEF/SDS/PAGE analysis of the rat brain mitochondria proteome

Assay conditions were as described in the Experimental section. Rat brain mitochondria were purified, subjected to 2D IEF/SDS/PAGE, and stained with SYPRO™ Ruby protein gel stain. On average ($n = 24$), approx. 580 individual spots could be detected. Straight lines on the left indicate the molecular masses and pI values (bottom border) of marker proteins, whereas arrows indicate molecular masses of mitochondrial proteins (pI values are shown above the top border), designated 1–7 (see Table 2).

Table 2   Designation of proteins identified following 2D IEF/SDS PAGE of rat brain mitochondria

Numbers refer to the designation of peptide spots on the two-dimensional gel shown in Figure 3. Accession numbers are from the SwissProt protein database. The theoretical molecular mass (M_r) and isoelectric point (pI) values of the mature proteins are shown. Proteins were identified by N-terminal sequencing and assigned on the basis of probability scores generated by BLAST analysis of SwissProt and/or SeqIt™ software (Array Genetics).

Spot no.	Protein name	Accession number	Species	Mitochondrial localization	$M_r \times 10^{-3}$	pI	Probability
1	ATP synthase β-chain	P10719	Rat	Inner membrane	51.71	4.95	High
2	Ubiquinol-cytochrome c reductase complex core protein 1	Q9CZ13	Mouse	Inner membrane	49.22	5.28	High
3	Pyruvate dehydrogenase E1 β subunit	P49432	Rat	Matrix	35.84	5.29	High
4	Hsp 60	P19226	Rat	Matrix	57.93	5.35	High
5	Hsp 70	P48721	Rat	Matrix	68.85	5.51	High
6	Isovaleryl-CoA dehydrogenase	P12007	Rat	Matrix	43.097	6.12	Medium
7	ATP synthase α-chain	P15999	Rat	Inner membrane	55.27	8.28	Medium

7.0 (Figure 4A). Spot 4 is situated near pH 7 and exhibits a molecular mass of about 80 kDa. Immunoblot analysis using anti-(phospho-Tyr) antibody detected immunoreactive spots with the same co-ordinates as the radioactively labelled peptides 1, 2, 3 and 4, thus indicating that these peptides contain ^{32}P-Tyr residues (results not shown). The addition of arJNK1 to the mitochondrial suspension resulted in the appearance of seven new, clearly identifiable, radioactive signals, designated A, B, C, D, E, F and G (Figure 4B). Furthermore, Figure 4(B) demonstrates an increase in the density of spot 4, which was already present

in the control. The other control signals (1, 2 and 3) were also present in the JNK-treated mitochondria but exhibited no significant changes with regard to density. Spots A and B are localized near pH 7 and between pH 4.5 and 5.1, respectively, and have a molecular mass of less than 31 kDa (Figure 4B). When parallel two-dimensional gels were immunoblotted with anti-Bcl-2 and anti-Bcl-x_L pAbs, immunoreactive peptides with the same co-ordinates as the radioactive spots A and B were detected, strongly indicating that spots A and B represent the proteins Bcl-2 and Bcl-x_L respectively (results not shown). These findings are
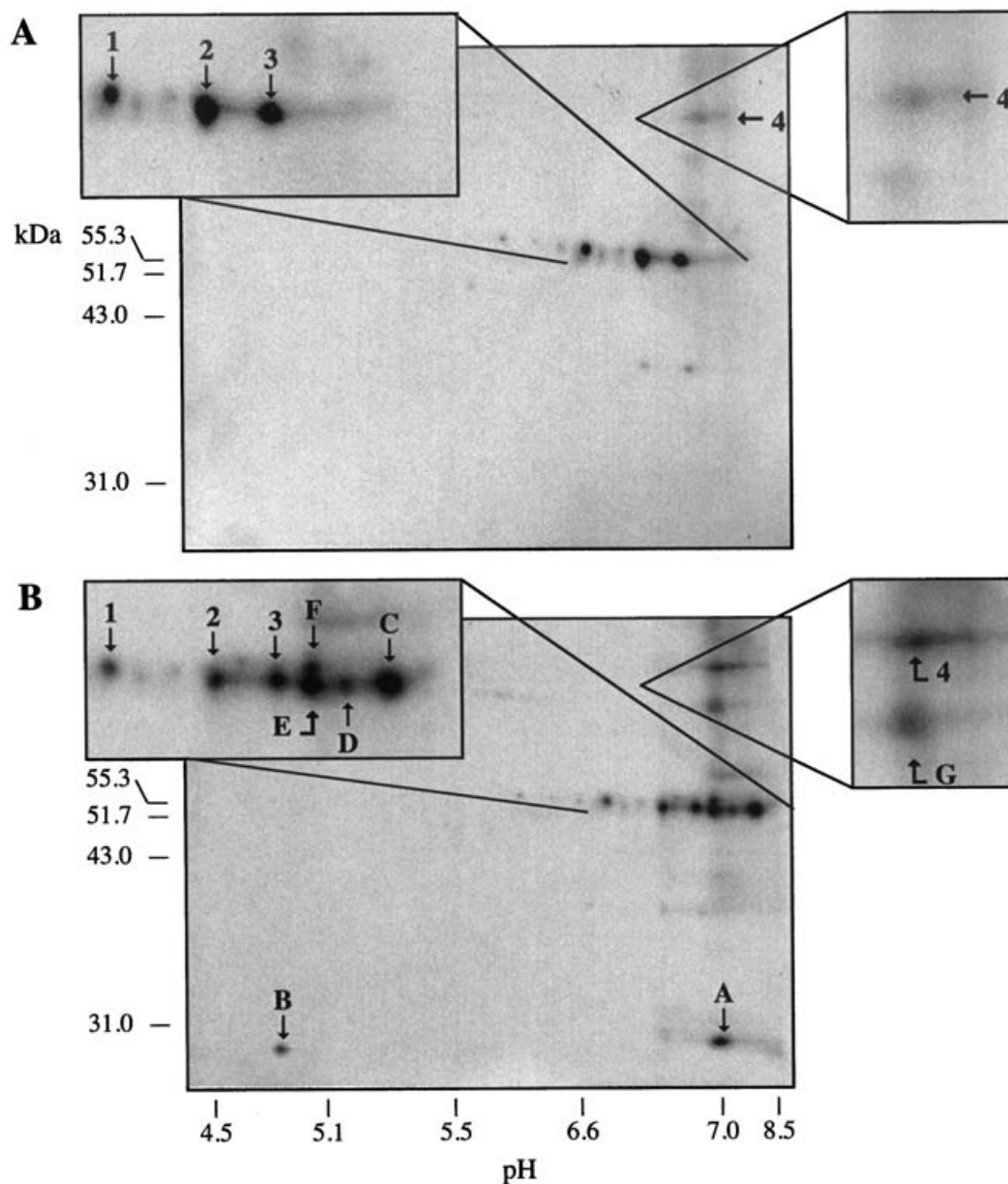
Figure 4   JNK-catalysed phosphorylation of mitochondrial proteins

Assay conditions were as described in the Experimental section. Rat brain mitochondria were incubated with recombinant JNK1 in the presence of $[\gamma\text{-}^{32}\text{P}]$ATP, subjected to 2D IEF/SDS/PAGE and analysed by autoradiography. (**A**) Representative autoradiogram obtained using inactive rJNK1 as a control: it shows the presence of four radioactively labelled peptides, designated 1–4. Spots 1–3 represent peptides with an approximate molecular mass of 55 kDa and are located in the pH range 6.6–7.0. Spot 4 is situated near pH 7 and exhibits a molecular mass of about 80 kDa. (**B**) Incubation with arJNK1 resulted in the appearance of 11 radioactive peptides, including spots 1–4 (found also in the control) and new signals designated A–G. Spots A and B are located near pH 7 and between pH 4.5 and 5.1 respectively and have molecular masses of less than 31 kDa. The radioactive peptides C–F have molecular masses of approx. 55 kDa and are located between pH 7.0 and 8.5. Spot G exhibits a molecular mass of approx. 76 kDa and a pI value near 7.0.

supported by the molecular masses and pI values as provided by Swiss-Prot (release 40.37), listing the molecular masses for Bcl-2 (rat; accession no. P49950) and Bcl-x_L (rat; P53563) as 26.6 and 26.2 kDa respectively. The pI values obtained from the same source correlate to 7.06 for Bcl-2 and 4.87 for Bcl-x_L. The other radioactive peptides C, D, E and F have molecular masses of approx. 55 kDa and are located in a pH range between 7.0 and 8.5 (Figure 4B). Spot G exhibits a molecular mass of around 76 kDa and a pI near 7.0 (Figure 4B). Control experiments using anti-JNK1 pAb excluded the possibility that these peptides

originated from autophosphorylated arJNK1; furthermore the molecular mass of arJNK1 is approx. 43 kDa (manufacturer's information, from Upstate Biotechnology), which is significantly lower than the mass of the observed radioactive peptides (see above).

Although the identity of the mitochondrial peptides radioactively labelled following exposure of isolated mitochondria to active JNK could not be ascertained conclusively, it becomes apparent that JNK-mediated post-translational modification of mitochondrial proteins is not limited to Bcl-2 and Bcl-x_L.
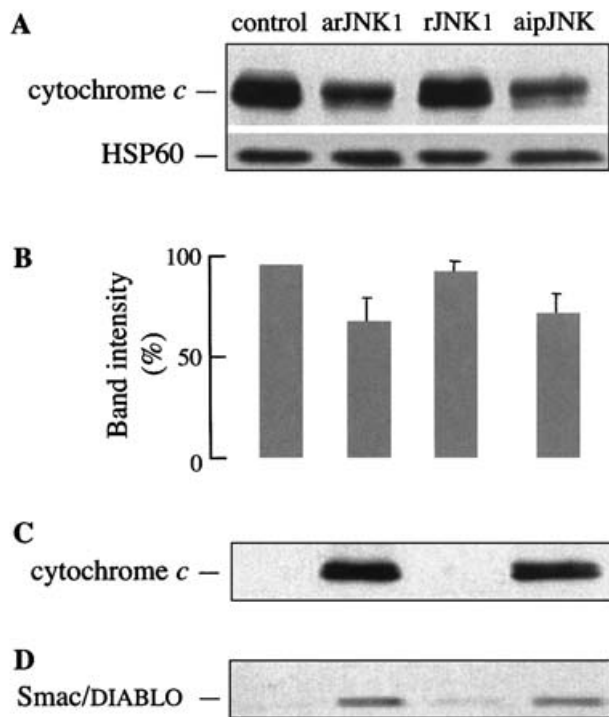
Figure 5   JNK mediates the release of the pro-apoptotic cytochrome *c* from isolated mitochondria

Assay conditions were as described in the Experimental section. Rat brain mitochondria were incubated with arJNK1/rJNK1 and aipJNK in the presence of ATP. (**A**) Western immunoblot of mitochondrial pellet. (**B**) Semi-quantitative analysis (densitometry) of data in (**A**); data are from four independent experiments. (**C**) Western immunoblot of cytochrome *c* in supernatant. (**D**) Western immunoblot of Smac/DIABLO in supernatant.

Active JNK facilitates release of pro-apoptotic factors from mitochondria

JNK activation, Bcl-2 phosphorylation and the release of cytochrome *c* seem to proceed in parallel during apoptosis. The mechanisms linking these events are unclear and the function of Bcl-2 phosphorylation in terms of loss or gain of anti-apoptotic potential remains incompletely defined. In these studies, intact, coupled and bioenergetically competent mitochondria were incubated in the presence of active or inactive JNK for 30 min. The results in Figure 5 show that arJNK1 and aipJNK induced a significant release of cytochrome *c* from isolated rat brain mitochondria. Semi-quantitative measurements on the basis of densitometric analyses of the obtained Western immunoblots indicated that JNK mediates the release of approx. 30 % ($n = 4$) of total cytochrome *c* under these conditions (Figures 5A and 5B). Analysis of the freeze-dried supernatants confirmed that active JNK, but not inactive JNK (rJNK1), facilitated cytochrome *c* release into the extra-mitochondrial medium (Figure 5C). It is noteworthy that although the supernatant did not contain mitochondrial matrix proteins, such as Hsp60, Western immunoblot analysis revealed the presence of Smac/DIABLO in the supernatant of arJNK1/aipJNK-treated mitochondria (Figure 5D).

With regard to the dynamics of JNK-mediated release of cytochrome *c*, early results indicated that a 10 min incubation of mitochondria with either arJNK1 or aipJNK did not result in a release of cytochrome *c*, as could be concluded from the Western immunoblot analysis of mitochondrial pellets and supernatants
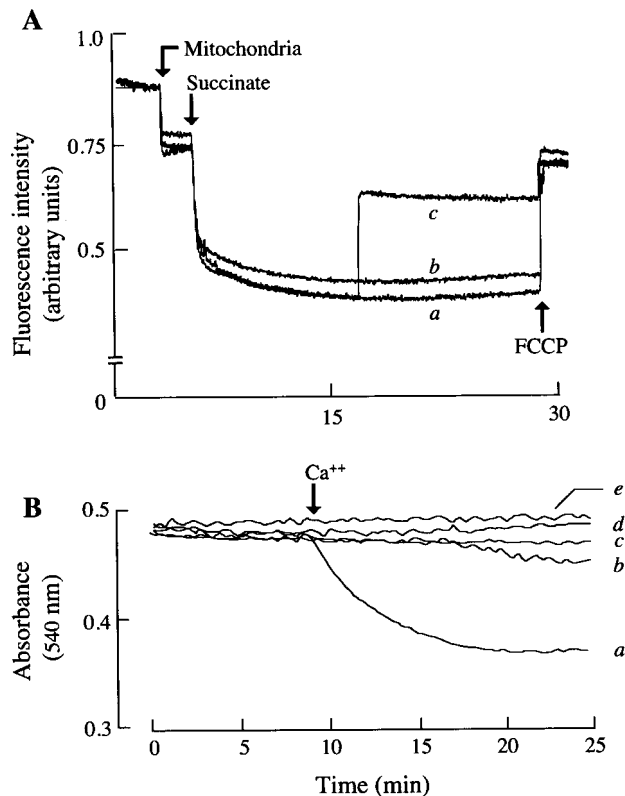
Figure 6   JNK modulates mitochondria function

(**A**) Time course of changes in $\Delta\psi$m: effect of JNK. Assay conditions: rat brain mitochondria (1 mg of protein/ml), oligomycin (5 μM), rotenone (5 μM) and TMRM (0.5 μM) in the assay buffer described in the Experimental section were supplemented with succinate (5 mM) and FCCP (0.5 μM) where indicated by the arrows. Trace a, control; trace b, plus rJNK (0.3 ng/μl); trace c, plus arJNK1 (0.3 ng/μl). Traces are representative of six independent experiments. (**B**) Time course of Ca^{2+}-induced mitochondrial swelling. Assay conditions: rat brain mitochondria (1 mg of protein/ml) in assay buffer were supplemented with Ca^{2+} (150 μM) and absorbance followed at 540 nm. Trace a, control; trace b, plus arJNK1 (0.3 ng/μl) added 15 min prior to Ca^{2+} addition; trace c, plus FCCP (0.5 μM); trace d, plus arJNK1 (0.3 ng/μl; no Ca^{2+} addition); trace e, plus CsA (5 μM). Traces are representative of four independent experiments.

(results not shown). Taken together, these results strongly support the notion that JNK induces the release of cytochrome *c* from mitochondria, thus initiating a major step in the execution of apoptosis.

Active JNK modulates mitochondrial function

As ascertained above, JNK phosphorylated various mitochondrial proteins, including Bcl-2 and Bcl-x$_L$, and facilitated the release of pro-apoptotic factors from isolated rat brain mitochondria. In order to obtain information with regard to a potential mechanistic explanation for the earlier observations, the effects of active JNK on the $\Delta\psi$m as well as mitochondrial swelling were investigated.

The putative JNK-dependent modulation of the $\Delta\psi$m was assessed by measuring the $\Delta\psi$m-dependent distribution of the fluorescent probe TMRM. The addition of isolated mitochondria to a buffer containing TMRM resulted in a decrease in fluorescence under control conditions, as this compound partitions into the mitochondria (Figure 6A, trace a). The supplementation with succinate energized mitochondria and increased $\Delta\psi$m, which in turn facilitated $\Delta\psi$m-driven TMRM accumulation within the mitochondrial compartment, subsequently leading to a further decrease in fluorescence (Figure 6A, trace a). The addition of

FCCP at the end of the experiment collapsed $\Delta\psi$m, consequently leading to a redistribution of TMRM as seen by an increase in fluorescence (Figure 6A, trace a). Hence FCCP represents an internal control because the fluorescence measured following its addition reflects the passive TMRM distribution and thus should be comparable with the non-energized condition (Figure 6A, trace a). The supplementation of inactive rJNK1 into the system described above had no effects on $\Delta\psi$m (Figure 6A, trace b). However, arJNK1 (added at time 0) induced a drastic decrease in $\Delta\psi$m (Figure 6A, trace c). Although the degrees of change in $\Delta\psi$m were not subject to significant inter-assay variation ($n = 6$), the incubation time required for the change to occur ranged between 10 and 15 min. It is noteworthy that the JNK-mediated decline of $\Delta\psi$m was CsA-independent (results not shown) and did not represent a complete collapse of $\Delta\psi$m as demonstrated by the ability of FCCP to further facilitate decrease (Figure 6A, trace c).

The swelling of mitochondria, a colloidosmotic process observed *in vitro*, is often used as a model of the imPT. To examine whether or not active JNK triggers the assembly and subsequent opening of the imPT pore, mitochondria were exposed to arJNK1/aipJNK/rJNK1 under conditions previously shown to be conducive to mitochondrial swelling induced by Ca^{2+} [34]. The addition of Ca^{2+} to a suspension of isolated mitochondria was used as a positive control and, as anticipated, induced mitochondrial swelling (Figure 6B, trace a). Ca^{2+}-induced swelling was completely inhibited by the prior addition of CsA, a modulator of cyclophilin D and potent inhibitor of the imPT (Figure 6B, trace e). Cyclophilin D-sensitive Ca^{2+}-induced imPT is believed to represent a regulated mPT pore formation and permeability transition of the inner membrane. The addition of arJNK1 to isolated mitochondria was not sufficient to trigger swelling (Figure 6B, trace d). Interestingly, the addition of active JNK (arJNK1), 15 min prior to Ca^{2+}, strongly abrogated Ca^{2+}-induced imPT (Figure 6B, trace b). As a control that the above-reported JNK-mediated depolarization of $\Delta\psi$m was responsible for the attenuation of Ca^{2+}-induced swelling, FCCP was used to depolarize the $\Delta\psi$m prior to Ca^{2+} addition. In concurrence with previous reports [35], these results showed that the presence of $\Delta\psi$m was essential for Ca^{2+}-induced swelling in the model used here (Figure 6B, trace c). Collectively, the results demonstrate that active JNK exerts a profound effect on the bioenergetic properties and the functional integrity of mitochondria.

DISCUSSION

The JNK signal-transduction pathway is implicated in many physiological and pathological conditions and appears to be essential for the execution of apoptosis in response to several different stimuli [20]. However, the molecular mechanisms that may account for a role of JNK in mitochondria-dependent apoptotic signal transduction remain the subject of discussion. The purpose of this investigation was to clarify the potential biological role of mitochondria as an important cellular target of pro-apoptotic JNK signalling. The data obtained in this study on isolated rat brain mitochondria, using arJNK as well as aipJNK protein, support earlier reports that active JNK mediates the release of pro-apoptotic proteins from mitochondria, such as cytochrome c and Smac. This effect does not depend on JNK-induced *de novo* protein expression. Evaluations of cytochrome c release revealed that active JNK facilitated a partial loss of cytochrome c, which might reflect either a partial release of cytochrome c from all mitochondria in suspension or a complete cytochrome c loss from a particular sub-population. This study also demonstrated that the JNK-induced phosphorylation

of mitochondrial Bcl-2 and Bcl-x_L was independent of other cytosolic mediator kinases. More importantly, the data herein strongly indicate new, so far unidentified, protein targets for JNK within mitochondria.

The proposed consequences of JNK signalling targeted towards mitochondria are represented by the release of pro-apoptotic factors. Two essential principles culminating in cytochrome c release from mitochondria may be hypothesized: (i) imPT and (ii) omPT. The former, imPT, is thought to require the assembly of the imPT-pore complex constituted by various proteins including, but not limited to, ANT, VDAC and cyclophilin D [36]. It has been proposed that imPT-pore opening would cause an influx of low-molecular-mass solutes from the cytosol (or the suspension buffer *in situ*) into the matrix, leading to swelling and rupture of the outer mitochondrial membrane and the release of pro-apoptotic proteins [36]. Ca^{2+} has been identified as the single most important activator of imPT-pore formation [37]. However, because of the relatively high concentrations required for Ca^{2+}-induced imPT, its significance in a cellular context [30] remains unclear. With regard to the latter principle, omPT, it has been postulated that the formation of outer-membrane pores may enable the release of intermembrane space proteins, such as cytochrome c [36,38]. VADC, pro-apoptotic Bcl-2 family members, like Bax, or cytosolic caspases have been suggested to participate in pore formation, facilitating omPT [36,38].

The mechanisms of both omPT and imPT can be functionally linked to the $\Delta\psi$m; thus factors influencing $\Delta\psi$m become important with regard to permeability transition. In terms of omPT, VADC is a likely candidate for $\Delta\psi$m-dependent function and it has been shown that $\Delta\psi$m is a major regulatory determinant for maintaining a particular pore size of VDAC [39]. This could have important implications for the temporal sequence of events relating to omPT and cytochrome c release during apoptosis. With regard to the imPT, it has been demonstrated that an $\Delta\psi$m-dependent electrogenic uniporter, which controls the transport of Ca^{2+} into the matrix and thus the first step necessary for imPT pore formation, is situated within the inner membrane [36,38,40]. Hence, it becomes apparent that the Ca^{2+}-induced imPT may crucially depend on $\Delta\psi$m.

The results shown here demonstrated that active JNK led to a partial collapse of $\Delta\psi$m. It might be argued that the JNK-mediated decrease of $\Delta\psi$m occurred independently of imPT, because (i) this effect was CsA-independent, (ii) JNK itself did not induce mitochondrial swelling and (iii) JNK, like FCCP, attenuated Ca^{2+}-induced swelling. If this argument were tenable, the observed release of cytochrome c induced by JNK would depend on the omPT. Thus the question arises as to what triggered omPT? An essential key in answering this question might be provided by focusing on the possible sequence of events: (i) JNK mediated a release of cytochrome c, subsequently culminating in a collapse of $\Delta\psi$m; (ii) JNK induced a decrease in $\Delta\psi$m, which subsequently lead to omPT and cytochrome c release. With regard to (i), experiments incorporating Bax into the outer membrane of mitochondria, thus constituting a possible model of omPT, suggested that the pores formed by Bax mediated the release of cytochrome c, subsequently leading to a collapse of $\Delta\psi$m [36,38]. In this scenario, it is likely that cytochrome c release precedes the collapse of $\Delta\psi$m. As suggested previously, Bax-induced cytochrome c release may be based on channel formation [38] or interaction with proteins like VDAC [9]. In this context, it was proposed that Bcl-2/Bcl-x_L, present in the outer mitochondrial membrane, exerted their anti-apoptotic effects by inhibiting omPT through the binding/inactivating of pro-apoptotic Bcl-2 members, like Bax [4,8]. This view brings forward a biological role for the JNK-catalysed phosphorylation of

Bcl-2/Bcl-x_L, because the phosphorylation of Bcl-2 has been shown to abrogate binding to Bax (and other Bcl-2 members) and to inhibit anti-apoptotic properties [5,11]. However, this model relies on the presence of Bax or other channel-forming pro-apoptotic Bcl-2 family members. *In vivo* Bax translocates from the cytosol to the mitochondria following an apoptotic stimulus. This possibility can be excluded in our model using isolated mitochondria. Although Bax was present within isolated rat brain mitochondria (results not shown), the levels were low compared with those of Bcl-2 and it remains uncertain as to whether or not phosphorylation of Bcl-2/Bcl-x_L would have freed enough Bax to form channels or to modulate the function of proteins like VDAC.

Regarding event (ii), the second sequence of events proposed above, the findings herein indicate that JNK facilitated the decrease of $\Delta\psi$m following an incubation of 10–15 min. However, no cytochrome c release from mitochondria could be detected following a 10 min exposure to active JNK. Thus it might be hypothesized that in our model the partial collapse of $\Delta\psi$m preceded cytochrome c release. This hypothesis would be dependent on the ability of JNK to impact directly on $\Delta\psi$m through the phosphorylation of regulatory sites of the electron-transport chain or indirectly via mitochondrial mediator kinases/phosphatases. Kinase-mediated modulations of $\Delta\psi$m have been described with regard to cAMP/protein kinase A-mediated phosphorylation of different subunits of complex I [41] or the phosphorylation of distinct serine residues on cytochrome c oxidase [42]. A role for JNK as a regulator of $\Delta\psi$m, however, has not yet been documented. Therefore JNK-dependent phosphorylation of mitochondrial proteins other than Bcl-2/Bcl-x_L may represent a potential mechanism for the modulation of mitochondrial functions during apoptosis.

In a cellular context, the importance of mitochondria as a primary target for JNK-dependent apoptotic processes, which are independent of *de novo* protein expression, becomes increasingly apparent and is supported by the following observations. (i) JNK is activated and subsequently translocates to mitochondria following different apoptotic stimuli [43]. (ii) Sab (SH3BP5), a new JNK-interacting protein, associates with mitochondria and thus targets JNK to this compartment [44]. (iii) An inhibition or knockout of JNK has resulted in the inability to execute mitochondrion-dependent apoptosis [45]. (iv) A modulation of Bcl-2 phosphorylation sites prevented JNK-catalysed phosphorylation and abrogated cell death [13].

It is worth noting that the new view of regulation of mitochondrial respiration involves the availability of ADP to the ATPase F_1 complex and of oxygen and NO to cytochrome oxidase [46]. The latter, NO, binds reversibly to cytochrome oxidase with high affinity, modulates oxygen uptake, and increases the mitochondrial production of H_2O_2 [47]. NO can be generated by the mitochondrial nitric oxide synthase [48]. Accordingly, activation of this enzyme may be followed by an increase in the mitochondrial production of H_2O_2 [47], which may be considered a pleiotropic signal involved in the regulation of different cellular processes, among them JNK signalling [49]. NO diffusing from mitochondria may also modulate (inactivate) JNK1 via S-nitrosylation [50]. Hence, NO and H_2O_2, generated and released by mitochondria, are involved in a delicate balance leading to modulation of JNK activity.

Taken together, JNK is a competent inducer of cytochrome c release from the intermembrane space of mitochondria, thus initiating an essential step in mitochondrion-dependent apoptosis. This study suggests that JNK mediates its pro-apoptotic effect through the initiation of omPT, rather than imPT. This notion is supported by the following. First, JNK-induced cytochrome c release was independent of imPT and CsA-insensitive. Secondly,

JNK mediated a partial collapse of $\Delta\psi$m in an imPT- and CsA-independent manner. Thirdly, JNK was unable to induce imPT/swelling and did not act as a co-inducer, but as an inhibitor of Ca^{2+}-induced imPT. Fourthly, JNK phosphorylated Bcl-2/Bcl-x_L, proteins that have previously been implicated in omPT. Furthermore, the new as-yet-unidentified protein targets for JNK within mitochondria may represent critical mediators for JNK-dependent modulations of bioenergetical parameters of mitochondria during apoptosis.

REFERENCES

1   Hengartner, M. O. (2000) The biochemistry of apoptosis. Nature (London) **407**, 770–775

2   Thompson, C. B. (1995) Apoptosis in the pathogenesis and treatment of disease. Science **267**, 1456–1462

3   Yuan, J. and Yankner, B. A. (2000) Apoptosis in the nervous system. Nature (London) **407**, 802–809

4   Adams, J. M. and Cory, S. (1998) The Bcl-2 protein family: arbiters of cell survival. Science **281**, 1322–1326

5   Antonsson, B. and Martinou, J. C. (2000) The Bcl-2 protein family. Exp. Cell Res. **256**, 50–57

6   Korsmeyer, S. J. (2000) Activation and inactivation of BCL-2 members. FASEB J. **14**, A1404-A1404

7   Veis, D. J., Sorenson, C. M., Shutter, J. R. and Korsmeyer, S. J. (1993) Bcl-2-deficient mice demonstrate fulminant lymphoid apoptosis, polycystic kidneys, and hypopigmented hair. Cell **75**, 229–240

8   Cheng, E. H. Y. A., Wei, M. C., Weiler, S., Flavell, R. A., Mak, T. W., Lindsten, T. and Korsmeyer, S. J. (2001) BCL-2, BCL-X-L sequester BH3 domain-only molecules preventing BAX- and BAK-mediated mitochondrial apoptosis. Mol. Cell **8**, 705–711

9   Shimizu, S., Narita, M. and Tsujimoto, Y. (2000) BcL-2 family proteins regulate the release of apoptogenic cytochrome c by the mitochondrial channel VDAC. Nature (London) **399**, 483–487

10 Brenner, C., Cadiou, H., Vieira, H. L. A., Zamzami, N., Marzo, I., Xie, Z. H., Leber, B., Andrews, D., Duclohier, H., Reed, J. C. and Kroemer, G. (2000) Bcl-2 and Bax regulate the channel activity of the mitochondrial adenine nucleotide translocator. Oncogene **19**, 329–336

11 Chang, B. S., Minn, A. J., Muchmore, S. W., Fesik, S. W. and Thompson, C. B. (1997) Identification of a novel regulatory domain in Bcl-x(L) and Bcl-2. EMBO J. **16**, 968–977

12 Ito, T., Deng, X. M., Carr, B. and May, W. S. (1997) Bcl-2 phosphorylation required for anti-apoptosis function. J. Biol. Chem. **272**, 11671–11673

13 Srivastava, R. K., Mi, Q. S., Hardwick, J. M. and Longo, D. L. (1999) Deletion of the loop region of Bcl-2 completely blocks paclitaxel-induced apoptosis. Proc. Natl. Acad. Sci. U.S.A. **96**, 3775–3780

14 Yamamoto, K., Ichijo, H. and Korsmeyer, S. J. (1999) BCL-2 is phosphorylated and inactivated by an ASK1/Jun N-terminal protein kinase pathway normally activated at G(2)/M. Mol. Cell. Biol. **19**, 8469–8478

15 Ling, Y. H., Tornos, C. and Perez-Soler, R. (1998) Phosphorylation of Bcl-2 is a marker of M phase events and not a determinant of apoptosis. J. Biol. Chem. **273**, 18984–18991

16 Attalla, H., Westberg, J. A., Andersson, L. C., Adlercreutz, H. and Makela, T. P. (1998) 2-methoxyestradiol-induced phosphorylation of Bcl-2: Uncoupling from JNK/SAPK activation. Biochem. Biophys. Res. Commun. **247**, 616–619

17 Tseng, C. J., Wang, Y. J., Liang, Y. C., Jeng, J. H., Lee, W. S., Lin, J. K., Chen, C. H., Liu, I. C. and Ho, Y. S. (2002) Microtubule damaging agents induce apoptosis in HL 60 cells and G2/M cell cycle arrest in HT 29 cells. Toxicology **175**, 123–142

18 Blagosklonny, M. V., Chuman, Y., Bergan, R. C. and Fojo, T. (1999) Mitogen-activated protein kinase pathway is dispensable for microtubule-active drug-induced Raf-1/Bcl-2 phosphorylation and apoptosis in leukemia cells. Leukemia **13**, 1028–1036

19 Maundrell, K., Antonsson, B., Magnenat, E., Camps, M., Muda, M., Chabert, C., Gillieron, C., Boschert, U., VialKnecht, E., Martinou, J. C. and Arkinstall, S. (1997) Bcl-2 undergoes phosphorylation by c-Jun N-terminal kinase stress-activated protein kinases in the presence of the constitutively active GTP-binding protein Rac1. J. Biol. Chem. **272**, 25238–25242

20   Davis, R. J. (2000) Signal transduction by the JNK group of MAP kinases. Cell **109**, 239–252

21   reference deleted

22   Fan, M. Y., Goodwin, M., Vu, T., Brantley-Finley, C., Gaarde, W. A. and Chambers, T. C. (2000) Vinblastine-induced phosphorylation of Bcl-2 and Bcl-XL is mediated by JNK and occurs in parallel with inactivation of the Raf-1/MEK/ERK cascade. J. Biol. Chem. **275**, 29980–29985

23   Deng, X. M., Xiao, L., Lang, W. H., Gao, F. Q., Ruvolo, P. and May, W. S. (2001) Novel role for JNK as a stress-activated Bcl2 kinase. J. Biol. Chem. **276**, 23681–23688

24   Breitschopf, K., Haendeler, J., Malchow, P., Zeiher, A. M. and Dimmeler, S. (2000) Posttranslational modification of Bcl-2 facilitates its proteasome-dependent degradation: Molecular characterization of the involved signaling pathway. Mol. Cell. Biol. **20**, 1886–1896

25   Anderson, M. F. and Sims, N. R. (2000) Improved recovery of highly enriched mitochondrial fractions from small brain tissue samples. Brain Res. Protoc. **5**, 95–101

26   Swanson, M. A. (1950) Phosphatases of liver: I. Glucose-6-phosphatase. J. Biol. Chem. **184**, 647–659

27   Sottocasa, G. L., Kuylenstierna, B., Ernster, L. and Bergstrand, A. (1967) An electron-transport system associated with the outer membrane of liver mitochondria. A biochemical and morphological study. J. Cell Biol. **32**, 415–438

28   Dunkley, P. R., Baker, C. M. and Robinson, P. J. (1986) Depolarization-dependent protein-phosphorylation in rat cortical synaptosomes – characterization of active protein-kinases by phosphopeptide analysis of substrates. J. Neurochem. **46**, 1692–1703

29   Scaduto, R. C. and Grotyohann, L. W. (1999) Measurement of mitochondrial membrane potential using fluorescent rhodamine derivatives. Biophys. J. **76**, 469–477

30   Kahlert, S. and Reiser, G. (2002) Swelling of mitochondria in cultured rat hippocampal astrocytes is induced by high cytosolic Ca^{2+} load, but not by mitochondrial depolarization. FEBS Lett. **529**, 351–355

31   Diaz Brinton, R., Chen, S., Montoya, M., Hsieh, D., Minaya, J., Kim, J. and Chu, H. P. (2000) The women's health initiative estrogen replacement therapy is neurotrophic and neuroprotective. Neurobiol. Aging **21**, 475–496

32   Schroeter, H., Williams, R. J., Matin, R., Iversen, L. and Rice-Evans, C. A. (2000) Phenolic antioxidants attenuate neuronal cell death following uptake of oxidized low-density lipoprotein. Free Radical Biol. Med. **29**, 1222–1233

33   Duncan, R. and Hershey, J. W. B. (1984) Evaluation of isoelectric-focusing running conditions during two-dimensional isoelectric-focusing sodium dodecyl sulfate-polyacrylamide gel-electrophoresis – variation of gel patterns with changing conditions and optimized isoelectric-focusing conditions. Anal. Biochem. **138**, 144–155

34   Jurgensmeier, J. M., Xie, Z. H., Deveraux, Q., Ellerby, L., Bredesen, D. and Reed, J. C. (1998) Bax directly induces release of cytochrome c from isolated mitochondria. Proc. Natl. Acad. Sci. U.S.A. **95**, 4997–5002

35   Aronis, A., Komarnitsky, R., Shilo, S. and Tirosh, O. (2002) Membrane depolarization of isolated rat liver mitochondria attenuates permeability transition pore opening and oxidant production. Antioxid. Redox Signaling **4**, 647–654

36   Zamzami, N. and Kroemer, G. (2001) The mitochondrion in apoptosis: how Pandora's box opens. Nat. Rev. Mol. Cell. Biol. **2**, 67–71

37   Crompton, M. (2000) Mitochondrial intermembrane junctional complexes and their role in cell death. J. Physiol. (Cambridge) **529**, 11–21

38   Crompton, M. (2000) Bax, Bid and the permeabilization of the mitochondrial outer membrane in apoptosis. Curr. Opin. Cell Biol. **12**, 414–419

39   Lemeshko, V. V. (2002) Model of the outer membrane potential generation by the inner membrane of mitochondria. Biophys. J. **82**, 684–692

40   Gunter, K. K. and Gunter, T. E. (1994) Transport of calcium by mitochondria. J. Bioenerg. Biomembr. **26**, 471–485

41   Papa, S., Scacco, S., Sardanelli, A. M., Petruzzella, V., Vergari, R., Signorile, A. and Technikova-Dobrova, Z. (2002) Complex I and the cAMP cascade in human physiopathology. Biosci. Rep. **22**, 3–16

42   Lee, I., Bender, E. and Kadenbach, B. (2002) Control of mitochondrial membrane potential and ROS formation by reversible phosphorylation of cytochrome c oxidase. Mol. Cell. Biochem. **234**, 63–70

43   Kharbanda, S., Saxena, S., Yoshida, K., Pandey, P., Kaneki, M., Wang, Q. Z., Cheng, K., Chen, Y. N., Campbell, A., Sudha, T. et al. (2000) Translocation of SAPK/JNK to mitochondria and interaction with Bcl-x(L) in response to DNA damage. J. Biol. Chem. **275**, 322–327

44   Wiltshire, C., Matsushita, M., Tsukada, S., Gillespie, D. A. F. and May, G. H. W. (2002) A new c-Jun N-terminal kinase (JNK)-interacting protein, Sab (SH3BP5), associates with mitochondria. Biochem. J. **367**, 577–585

45   Tournier, C., Hess, P., Yang, D. D., Xu, J., Turner, T. K., Nimnual, A., Bar-Sagi, D., Jones, S. N., Flavell, R. A. and Davis, R. J. (2000) Requirement of JNK for stress-induced activation of the cytochrome c-mediated death pathway. Science **288**, 870–874

46   Boveris, A. and Cadenas, E. (2000) Mitochondrial production of hydrogen peroxide regulation by nitric oxide and the role of ubisemiquinone. IUBMB Life **50**, 245–250

47   Brown, G. C. and Borutaite, V. (2001) Nitric oxide, mitochondria, and cell death. IUBMB Life **52**, 189–195

48   Elfering, S. L., Sarkela, T. M. and Giulivi, C. (2002) Biochemistry of mitochondrial nitric-oxide synthase. J. Biol. Chem. **277**, 38079–38086

49   Martindale, J. L. and Holbrook, N. J. (2002) Cellular response to oxidative stress: signaling for suicide and survival. J. Cell. Physiol. **192**, 1–15

50   Park, H. S., Park, E., Kim, M. S., Ahn, K., Kim, I. Y. and Choi, E. J. (2000) Selenite inhibits the c-Jun N-terminal kinase/stress-activated protein kinase (JNK/SAPK) through a thiol redox mechanism. J. Biol. Chem. **275**, 2527–2531